

Abstract

Geomagnetic indices are routinely used to characterize space weather event intensity. The D_{ST} index is well resolved, but is only available over 5 solar cycles. The aa index extends over 14 cycles but is highly discretized with poorly resolved extremes. We parameterize extreme aa activity by the annual averaged top few % of observed values, show these are exponentially distributed and they track annual D_{ST} index minima. This gives a 14 cycle average of $\sim 4\%$ chance of at least one great ($D_{ST} < -500nT$) storm and $\sim 28\%$ chance of at least one severe ($D_{ST} < -250nT$) storm per year. At least one $D_{ST} = -809$ $[-663, -955]nT$ event in a given year would be a 1:151 year event. Carrington event estimate $D_{ST} \sim -850nT$ is within the same distribution as other extreme activity seen in aa since 1868 so that its likelihood can be deduced from that of more moderate events. Events with $D_{ST} \lesssim -1000nT$ are in a distinct class, requiring special conditions.

Plain Language Summary

Here we use measurements of disturbances in the Earth's magnetic field that go back to 1868, and we present a novel way of analysing the data to identify the largest magnetic storms going back some 80 years longer than has been done before. As a result, we are able to state the chance of at least one super-storm occurring in a year. We find that on average there is a 4% (28%) chance of at least one great (severe) storm per year, and a 0.7% chance of a Carrington class storm per year, which can be used for planning the level of mitigation needed to protect critical national infrastructure.

1 Introduction

Extreme space weather events significantly disrupt systems for power distribution, aviation, communication and satellites; they are driven by large scale plasma structures emitted from the solar corona but their impact depends on a variety of factors [Baker & Lanzerotti, 2016]. Quantifying the chance of occurrence of extreme space weather events is essential to planning the resilience of vulnerable systems to catastrophic failure. Events that lead to geomagnetically induced currents that affect power grids are more likely close to solar maximum and in the descending phase of the solar cycle, but importantly they can occur at all other times in the solar activity cycle [Thomson et al., 2010]. The number of major solar eruptions varies with the approximately 11 year cycle of solar (sunspot) activity and with the amplitude of each solar cycle which is unique [Hathaway, 2015]. A particular concern is the possibility of a Carrington-class event, named after the space weather super-storm of 1859 [Tsurutani et al., 2003; Cliver & Svalgaard, 2004] which today could arguably cause severe disruption [Cannon et al., 2013; Daglis, 2004; Oughton et al., 2017].

Due to their rarity, amplitude and occurrence rates of space weather super-storms are challenging to quantify; it requires modelling based on the few observed large events. There have been a number of statistical studies, most of which rely on observations since the beginning of the space age. Estimates based on extrapolating a power law event distribution [Riley, 2012] suggest a 12% probability of a Carrington-class event in any given solar cycle, but are highly uncertain [Riley & Love, 2016]. A log-normal event distribution yields a much lower probability, again with a wide confidence interval [Love et al., 2015]. Estimates based on Extreme Value Theory [Thomson et al., 2011] also suggest the probability can be much lower [Siscoe, 1976; Silbergleit, 1996, 1999; Tsubouchi & Omura, 2007; Elvidge & Angling, 2018]. More moderate storms provide a larger set of observations. When storms across different solar cycles are aggregated, there is a well established correlation between occurrence rate and solar activity [Tsurutani et al., 2006; Tsubouchi & Omura, 2007]. Both solar wind driving [Tindale & Chapman, 2016, 2017] and geomagnetic activity [Hush et al., 2015; Chapman et al., 2018; Lockwood et al., 2018a]

64 track the differences in the level of activity at different phases of distinct solar cycles, and
65 between cycles of different intensity.

66 The above statistical studies are feasible for indices which are well resolved in ampli-
67 tude, such as D_{ST} . Whereas most indices, such as D_{ST} , are only available over the last
68 5 solar cycles, the aa index extends across 14 solar cycles- it is the longest almost contin-
69 uous record of changes in magnetic field across the earth's surface. Given the variability
70 in the amplitude of different solar cycles, it is desirable to obtain event occurrence rates
71 for this longer sample. However the aa index is by construction based on combining ob-
72 servations that are logarithmically discretized in amplitude and thus individual records of
73 the 3 hour aa index will have uncertainties that are both significant and non-trivial to esti-
74 mate [Bubenik & Fraser-Smith, 1977].

75 In this Letter we propose a parameterization of extreme aa activity using averages
76 of the annual top few % of observed records. Our goal is to use aa to obtain a proxy for
77 D_{ST} extremes that have occurred over the last 150 years. Our methodology is as follows.
78 We first show that there is a good linear correlation between the annual average of the top
79 few % values of aa and the annual D_{ST} minimum seen over the last 5 solar cycles. This
80 establishes a linear 'mapping' between the annual average of the top few % values of aa
81 and the annual D_{ST} minimum. We next use this linear mapping to convert these 150 an-
82 nual averages of the top few % of aa values into proxy D_{ST} extremes. This gives us 150
83 estimates for the annual minimum D_{ST} that occurred over the last 14 solar cycles of ac-
84 tivity. This record then provides an estimate of how many years have included super-storm
85 activity over the last 14 cycles, where super-storm activity is categorised in terms of the
86 largest annual event crossing a typical threshold minimum D_{ST} level. We find that the
87 largest samples are exponentially distributed. We can then determine the range of mini-
88 mum D_{ST} that would occur if this distribution applied to the next largest record in excess
89 of these 150 estimates, that is, a 1:151 year event. The Carrington event is also charac-
90 terised in terms of its excursion in D_{ST} and estimates vary considerably [Tsurutani et al.,
91 2003; Siscoe et al., 2006; Hayakawa et al., 2019]. We compare these estimates with the
92 range of minimum D_{ST} for a 1:151 event inferred from the 14 solar cycle proxy D_{ST} ex-
93 tremes record. This provides an assessment of whether the Carrington event was a more
94 intense version of the other super-storms that have occurred since 1868 or whether it was
95 in a class of its own, which would require the concurrence of special conditions in the
96 corona and solar wind and at the earth. Only if it is the former can we use the set of ob-
97 served storms to try to predict how likely such an event is in the future.

98 2 The datasets

99 Geomagnetic indices are derived from ground based magnetometer observations
100 [Mayaud, 1980] and are widely used to indicate the intensity of space weather events. The
101 D_{ST} index [Sugiura, 1964; Sugiura & Kamei, 1991] measures low-latitude global varia-
102 tions in the horizontal component of the geomagnetic field, thus representing the strength
103 of the equatorial ring current. The D_{ST} index is available [WDC, 2015] since 1957, so
104 that we can directly compare the aa index to D_{ST} over the last 5 solar cycles. The aa in-
105 dex is constructed [Mayaud, 1972] from the K indices determined at two antipodal obser-
106 vatories (invariant magnetic latitude 50 degrees) to provide a quantitative characterization
107 of magnetic activity, which is homogeneous through the whole series. An important con-
108 sideration is that the aa index (units, nT) is discretized in amplitude [Bubenik & Fraser-
109 Smith, 1977] since the underlying K index [Bartels et al., 1939] is a quasi-logarithmic 0-9
110 integer scale that characterizes the maximum positive and negative magnetic deviations
111 that occur during each 3 hour period at a given observatory.

112 We focus on the 3-hourly resolution aa index over the last 14 solar cycles, from
113 1868 to the present. This will be analysed alongside the daily sunspot number which is
114 available for the same time period. Recently Lockwood et al. [2018b,c] have produced a

115 homogenized 3-hourly *aa* index which has been corrected for secular changes in the in-
 116 trinsic geomagnetic field and the stations re-calibrated and then adjusted using a time-of-
 117 day/time-of-year dependent model of the stations' sensitivity. We have repeated the analy-
 118 sis here for both these versions of the *aa* index and key plots that use the homogenized *aa*
 119 index in the main sections of the Letter are reproduced using the 'classic' (ISGI) *aa* index
 120 in the SI. The homogenized *aa* index is available to end 2017 and our analysis extends up
 121 to this date, giving 150 calendar years of data.

122 **3 The *aa* index compared to D_{ST} at large values**

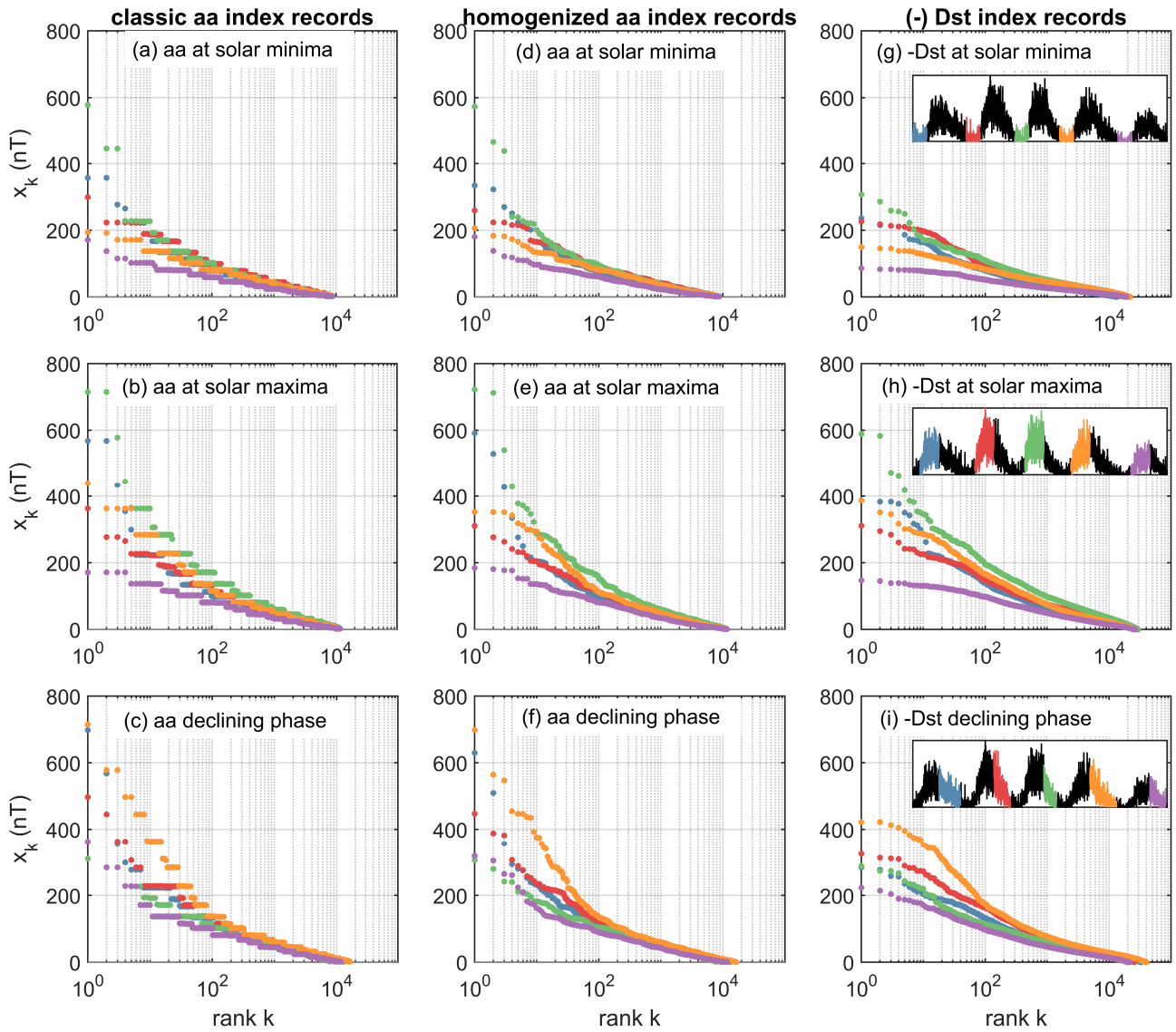
128 As the *aa* index is non-linearly and non-uniformly discretized in amplitude, we need
 129 to explore to what extent it can be used to characterize super-storms. We can see this by
 130 comparing it to $(-D_{ST})$, which is a well established measure of geomagnetic storm in-
 131 tensity. The D_{ST} index is well sampled in amplitude and therefore its maximum value
 132 does provide a meaningful estimate of super-storm intensity. Semilog rank order plots
 133 [Sornette, 2003] provide a method to display the behaviour of a set of values, particularly
 134 where they are large to extreme. The observations x_k are sorted in descending amplitude
 135 and plotted (ordinate) versus their rank k (abscissa), that is, the largest observed value is
 136 rank 1, the next largest, rank 2 and so on. Figure 1 compares rank order plots of the data
 137 records for $(-D_{ST})$ with that for classic and homogenized *aa* for the solar maximum in-
 138 terval, the solar minimum interval, and the declining phase of each of the last five solar
 139 cycles for which D_{ST} is available. We identify the intervals of solar minimum, solar maxi-
 140 mum and the declining phases by applying a single algorithm across the entire time series
 141 as detailed in the SI.

142 In Figure 1 it is immediately apparent that the classic *aa* amplitude is strongly dis-
 143 cretized at the high values, whereas $(-D_{ST})$ resolves them. The homogenized *aa* index
 144 shown in Figure 1 (d,e,f) does reduce some of this discretization. As *aa* combines obser-
 145 vations that are discretized in amplitude on a quasi-logarithmic scale, its maximum value
 146 (within a given interval, or event) does not quantify the extrema of geomagnetic distur-
 147 bances very well. As a consequence, *aa* is not readily amenable to standard analysis tech-
 148 niques for extracting, and quantifying the statistical properties of events or bursts. Thus
 149 whilst the Peak Over Threshold (POT) method has been successfully applied in quan-
 150 tifying the statistics of events in D_{ST} using Extreme Value Theory (e.g. [Tsubouchi &
 151 Omura, 2007]) it cannot simply be applied to the *aa* index. For this reason we will focus
 152 on year-long averages of the largest 0.5% and 5% *aa* records seen in each year as an es-
 153 timate of the relative level of extreme activity captured by the *aa* index. Figure 1 verifies
 154 that the large *aa* and $(-D_{ST})$ records do indeed both follow the variation within and be-
 155 tween solar cycles in the same manner despite the discretization present in the *aa* index.
 156 We can hence use *aa* to provide an indication of the variation in the extremes of geomag-
 157 netic activity over the last 14 solar cycles.

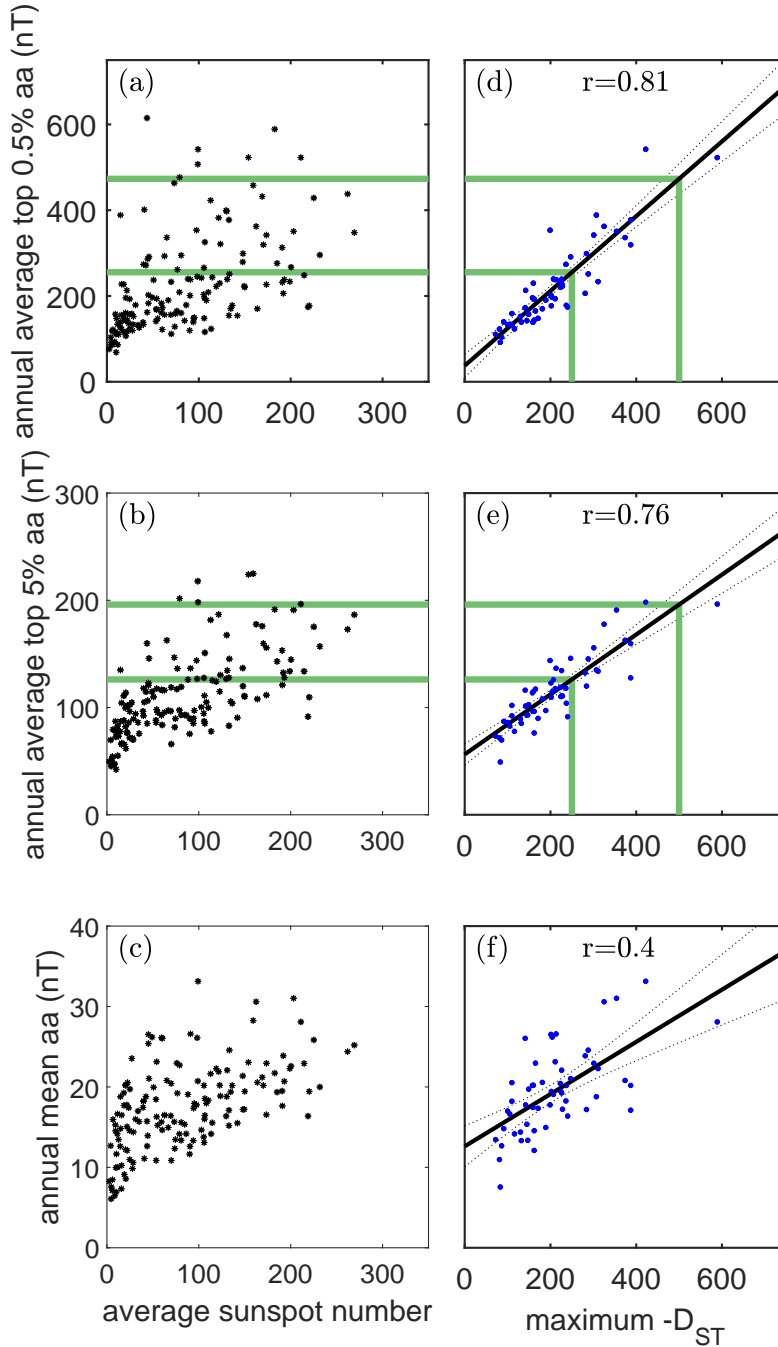
158 **4 Historical space weather activity**

170 Figure 2 plots the level of extreme activity captured by the homogenized *aa* index
 171 versus annual average sunspot number from 1868-2017 inclusive, corresponding to the last
 172 14 solar cycles. We parameterize extreme activity in *aa* by annual averages of the largest
 173 0.5 % (top panels), the largest 5 % (centre panels), and compare this with the average of
 174 all records (bottom panels). The averages are performed over non-overlapping calendar
 175 years. The left hand panels (a,b,c) of Figure 2 show the parameter space explored by *aa*
 176 and sunspot number over the last 14 solar cycles.

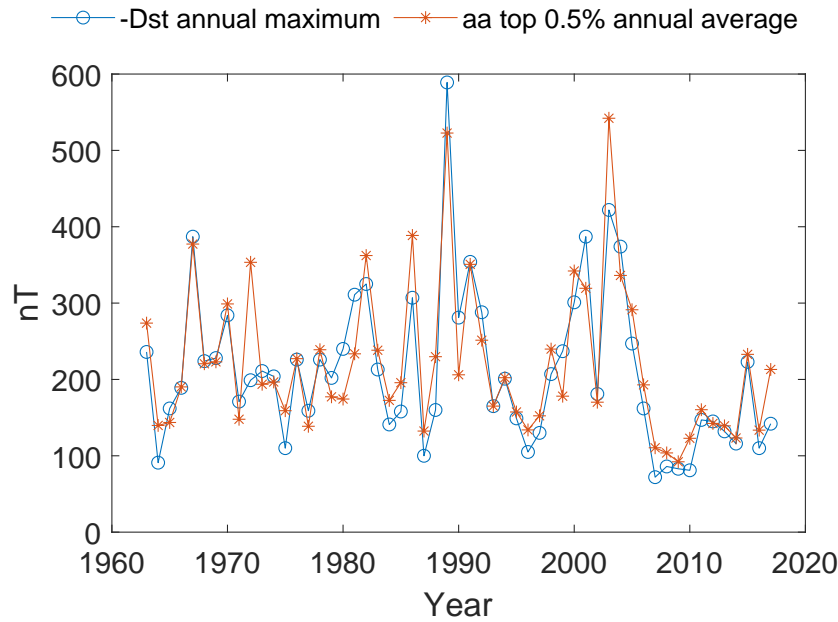
177 Fig 2 (c) reproduces the well known result [Feynman, 1982] that time averages of
 178 *aa* always exceed a baseline value which increases linearly with averaged sunspot number.
 179 A baseline can also be seen in the annual averages of the largest 0.5 % and the largest 5
 180 % *aa* values.



123 **Figure 1.** Rank order plots at the minima, maxima and declining phases of the last five solar cycles plotting
 124 data records for the classic *aa* index (a,b,c), the homogenized [Lockwood et al., 2018b,c] *aa* index (d,e,f) and
 125 $-D_{ST}$ index (g,h,i). The time interval from which data is used to form each rank order plot is indicated in the
 126 inset, overplotted on the daily sunspot number. Colours indicate the solar cycle 20 (blue) 21 (red) 22 (green)
 127 23 (orange) 24 (purple).



159 **Figure 2.** Panels (a-c) plot each value (black *) of the average of the largest 0.5 %, largest 5 % and all
 160 homogenized *aa* index records in each calendar year, versus average sunspot number, for all observations
 161 1868-2017 inclusive. The annual (calendar year) intervals are non-overlapping. Panels (d-f) plot (blue dots)
 162 the subset of the non-overlapping calendar year *aa* averages versus the maximum value of $-D_{ST}$ that oc-
 163 curred in the same year-long window, taken over the last five solar cycles. In each panel the solid black line
 164 plots the least squares fit and the dotted lines, the 0.95 confidence level of the fit, the r-squared coefficient for
 165 each fit is given on the panels. The green lines use this fit to map between D_{ST} thresholds of $-250nT$ and
 166 $-500nT$ and corresponding *aa* values.



167 **Figure 3.** Comparison between $(-)D_{ST}$ and homogenized aa across the last 5 solar cycles. The average of
 168 the largest 0.5 % homogenized aa index records in each calendar year (*) is plotted alongside the maximum
 169 $(-)D_{ST}$ (o) record that occurred in that year. The calendar year samples are non-overlapping.

181 We use the data from the last 5 solar cycles to obtain an approximate mapping be-
 182 tween values of extreme activity in D_{ST} and aa parameterized as above. We expect from
 183 Figure 1 that the large to extreme records of aa will track those of D_{ST} . As discussed
 184 above, the amplitude of D_{ST} is well resolved, so that we can consider the single observed
 185 minimum D_{ST} record that occurs in any given calendar year as a measure of the most se-
 186 vere storm that occurred in that year. Figure 3 overplots versus time the non-overlapping
 187 calendar year annual averages of the largest 0.5 % of the homogenized aa index with the
 188 maximum of $(-)D_{ST}$ that occurs in the same calendar year. We see that these quantities
 189 do track each other, albeit imperfectly. Figure 2, panel (d) plots (blue dots) these same
 190 quantities against each other, that is, the non-overlapping calendar year annual averages
 191 of the largest 0.5 % of the homogenized aa index are plotted versus the maximum of $(-)$
 192 D_{ST} that occurs in each calendar year as a scatter plot. Figures 2 (e,f) plot the analogous
 193 scatter plots for annual averages of the largest 5 %, and annual averages of aa . We then
 194 perform a least squares linear regression fit which is plotted as the solid black line, the .95
 195 confidence bounds are indicated by dotted lines. The r-squared coefficient of determina-
 196 tion (which indicates the proportionate amount of variation in the response variable ex-
 197 plained by the variable in the linear regression model) for each fit is given on the panels.
 198 Non-overlapping calendar year annual averages of the largest 0.5 % of the homogenized
 199 aa index (panel d) are well described by the linear least squares fit to annual minimum
 200 D_{ST} with r-squared coefficient of determination $r = 0.81$. The coefficients of this fitted
 201 line $a(x - b)$ are (with 95% confidence intervals) $a = 0.87 [0.76, 0.99]$ and $b = -43.12$
 202 $[-79.48, -6.76]$. The fit is reasonable, $r = 0.76$ for the largest 5 % (panel e). We need
 203 to choose a high threshold in order to isolate the largest events seen in each year of the
 204 aa index in order for these to be comparable with the largest annual minimum value of
 205 the D_{ST} index. This confirms that the correspondence is not strongly sensitive to the par-
 206 ticular choice of high threshold. As we would expect, the correspondence will be poor
 207 between the annual averages of aa and the largest annual minimum of D_{ST} and this is in-

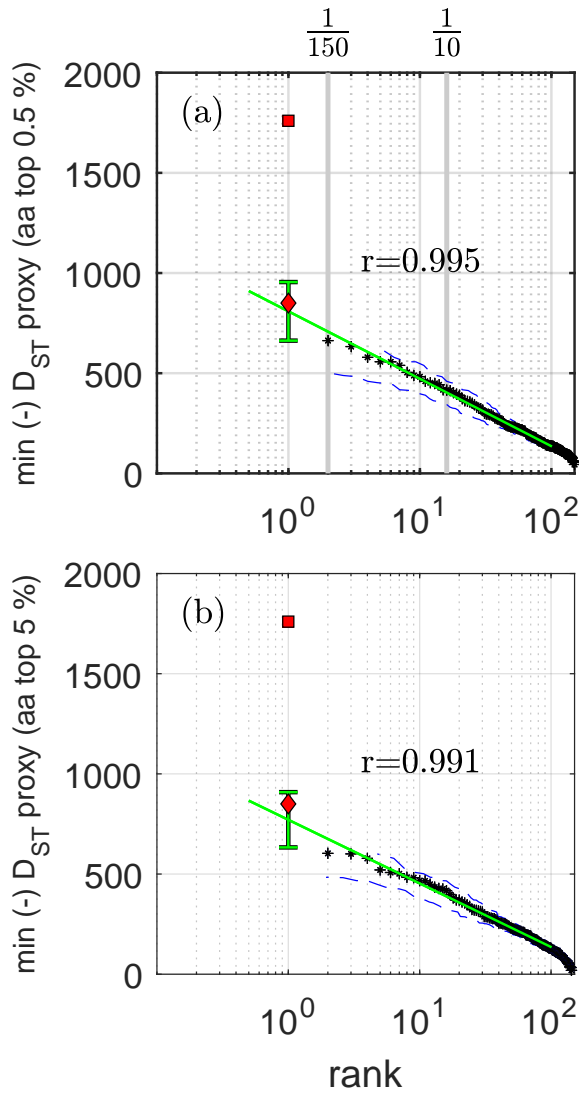
208 deed the case with $r = 0.4$ (panel f). We therefore focus on the annual averages of the
 209 largest few % of the *aa* index as the parameter for extreme activity.

218 We now use this least squares fit to read across between annual averages of the
 219 largest few % of *aa* records to the corresponding annual D_{ST} minimum ($(-)$ D_{ST} maxi-
 220 mum) values that would have been expected to occur over the last 14 solar cycles. Ex-
 221 treme space weather activity is often categorised in terms of D_{ST} crossing a minimum
 222 threshold. On Figure 2 we read across (green lines) D_{ST} levels of $-250nT$, the threshold
 223 for 'severe' [Riley & Love, 2016] and $-500nT$, the threshold for 'great' [Lakhina & Tsu-
 224 rutani, 2016] geomagnetic storms. D_{ST} levels of $(-250, -500)$ map onto the *aa* parameters
 225 as follows: annual averages of the largest 0.5 % of the homogenized *aa*: (255,473) and
 226 annual averages of the largest 5 % of the homogenized *aa* (126,196). Counting the points
 227 that lie above these thresholds in *aa* indicates that over 150 years, on average at least one
 228 great storm occurred in 6 (4 %) of those years, and at least one severe storm occurred in
 229 42 (28 %) of those years. These estimates average over any solar cycle variation.

230 We use the least squares fit in Figure 2 to read across from all 150 annual averages
 231 of the largest few % of *aa* records to the corresponding D_{ST} proxy, that is, the annual
 232 D_{ST} minimum ($(-)$ D_{ST} maximum) values that would have been expected to occur over
 233 the last 14 solar cycles. These are plotted in Figure 4 as rank order plots. In addition to
 234 the 150 annual D_{ST} proxy samples we have one additional sample that arguably exceeds
 235 all 150 values, that is, the Carrington event. The Carrington event estimate will therefore
 236 be rank 1 on this plot. The largest of the 150 annual D_{ST} proxy samples is plotted as rank
 237 2, the next largest as rank 3 and so on.

238 The dependencies seen on rank order plots are simply those of the distribution [Sor-
 239 nette, 2003] since an empirical estimate of the cumulative density function (cdf) $C(x_k)$ is
 240 obtained by plotting rank k normalized to the total number of samples, N , $C(x_k) = k/N$
 241 versus the samples x_k arranged in ascending order of size. The leading rank observation
 242 (rank 2 here) in 150 annual samples is then a 1/150 year event and we indicate this, and
 243 the location of a 1/10 year event across the top of the plot. To estimate the distribution
 244 functional form we have performed a least squares fit of a straight line on this semilog
 245 plot to the 100 largest ranked D_{ST} proxy samples. The green lines plot the fitted line
 246 $x_k = \beta(\log(k) - b)$ where $k = [2..101]$ is the rank. The r-square values for these fits
 247 is high, $r > 0.99$. For Panel (a) of Figure 4 the fit parameters with 95% confidence in
 248 brackets are $\beta = -146 [-148, -144]$ and $b = 5.53 [5.50, 5.56]$. The high r-square value
 249 of these fitted lines confirms that the tail of the distribution is well described by an expo-
 250 nential function [Sornette, 2003] $f(x) = (1/\beta)\exp(-x/\beta)$. The 95% confidence intervals
 251 for this fitted line give an uncertainty that deviates less than 1% from the fitted line. The
 252 dominant uncertainty on this plot arises from the variation between different empirical re-
 253 alisations of the cdf (or rank order plot) for which Greenwood [1926] provides an estimate
 254 as shown on the Figure. Applying this uncertainty to the results from Figure 4 then gives
 255 the chance of at least one great $D_{ST} < -500nT$ storm in a given year is then 4% with un-
 256 certainty bounds [0.9,7], and for a severe, $D_{ST} < -250nT$ storm is 28% [20,35]. The top
 257 ten most active years in the 150 year *aa* record (plotted as rank $k = 2..11$ on Figure 4)
 258 are summarised in Table 1. As we would expect, years in which some of the most severe
 259 storms occurred appear here, however we can now directly rank them and can estimate
 260 their % occurrence likelihood.

265 An important question is whether the Carrington event belongs to the same physi-
 266 cal class as the other super-storms. If so, its probable severity and chance of occurrence
 267 should be predictable at least in principle, as it will follow that of the other more mod-
 268 erate super-storms. If not, it is in a distinct physical class and past observations of more
 269 moderate super-storms may not inform estimates of its chance of occurrence; it is a 'Dragon
 270 King' [Sornette & Ouillon, 2012]. We now determine if estimates for the Carrington event
 271 are consistent with the exponential distribution of proxy D_{ST} . For an exponential we have
 272 [Sornette, 2003] an estimate of the fluctuations between one realization to another for the



210 **Figure 4.** The panels show rank order plots of non-overlapping annual minimum $(-D_{ST})$ proxy samples
 211 derived from: (a) the largest 0.5% and (b) the largest 5% of homogenized *aa* (black stars). The largest of
 212 these samples is plotted as rank 2, the next largest as rank 3 and so on. We plot as rank 1 two estimates of the
 213 Carrington event: $D_{ST} = -850nT$ (red diamond) and $D_{ST} = -1760nT$ (red square). The green lines indicates
 214 an exponential fit to the largest 100 values and the r -squared coefficient for each fit is given in the panels. The
 215 error bars for the the first ranked sample (green error bar) are estimated for an underlying exponential distri-
 216 bution (see text). The 95% confidence level for this empirical realization of the rank order plot are estimated
 217 from *Greenwood* [1926] (blue dashed lines).

Top ten most active years in the *aa* index record

rank	year	% chance per year	activity in that year
1	1921	0.67 [0, 1.9]	Remarkable storm ¹ ; Silverman & Cliver [2001], Table IV, VII ²
2	1938	1.33 [0, 3.1]	Fátima storm; Table III,IV,VII ²
3	2003	2.0 [0, 4.2]	Halloween storms; Weaver [2004], Table III ²
4	1946	2.67 [0.1, 5.2]	Table IV ²
5	1989	3.33 [0.5, 6.3]	Quebec power outage ¹ ; MacNeil [2018]; Table VII ²
6	1882	4.0 [0.9, 7.1]	Remarkable storm ¹ ; Love [2018], Table IV ²
7	1941	4.67 [1.3, 8.1]	geomagnetic storm; Love & Coïsson [2016]; Table III,IV ²
8	1909	5.33 [1.7, 8.9]	Remarkable storm ¹ ; Love et al. [2019a] Table IV, VII ²
9	1960	6.0 [2.2, 9.8]	Table III ²
10	1958	6.67 [2.7, 10.7]	Remarkable storm ¹ ; Table VII ²

261 **Table 1.** Rank ordering of the most active years with chance of occurrence from Figure 4. Remarkable
 262 storms¹(geomagnetic perturbation, Table 1 of Tsurutani et al. [2003]). Events² in Cliver & Svalgaard [2004]
 263 Tables III (fast transit events up to 2003), IV (Greenwich list of great storms up to 1954), VII (low latitude
 264 auroras up to 1958).

273 first ranked sample, it is $\pm\beta$. This is plotted as a green error bar on the rank 1 location of
 274 the exponential fit. This gives an estimate $D_{ST} = -809$ [−663, −955]. This is the range
 275 of values for D_{ST} for this event to be a 1 in 151 year event drawn from the same distri-
 276 bution as other extreme activity seen in *aa* over the last 14 solar cycles. We overplot at
 277 rank 1 the two estimates of the Carrington event (red diamond and square). From Figure
 278 4 we see that the estimate of $D_{ST} = -850nT$ is consistent with the above extrapolation
 279 of the exponential fit so that the likelihood of any given year exhibiting a Carrington-class
 280 event on this scale simply follows the exponential distribution that describes the other se-
 281 vere storms that have occurred since. However, a value of $D_{ST} = -1760nT$ (red square)
 282 is in its own class of behaviour, it is far from this exponential distribution tail.

283 We have parameterized extreme space weather activity with annual averages of the
 284 top few % of the *aa* index. Whilst this has allowed us to form a distribution from obser-
 285 vations over 14 solar cycles, it does not discriminate the statistics of individual events.
 286 This can only be done for time-series that are well resolved in amplitude, such as D_{ST} , for
 287 which there are a number of studies. We have identified a correspondence between the an-
 288 nual averages of the top few % of the *aa* index and the annual minimum D_{ST} , that is, the
 289 largest event in each year. In general, for moderate conditions, there will be several storms
 290 per year, so that the return period of a level of annual activity that we find here would
 291 not be expected to correspond to the return period for an event of a specific amplitude.
 292 For the most severe and infrequent storms there will be closer correspondence between
 293 these two measures. Our estimate that a $D_{ST} \sim -850nT$ is a ~ 1 in 150 year event is
 294 not inconsistent with that of Riley & Love [2016], a 10% [1,20] chance of occurrence per
 295 decade. The D_{ST} excursion $907 \pm 132nT$ Love et al. [2019b] estimate for the 1921 event
 296 also overlaps with the range determined here for the rank 1 event. Tsubouchi & Omura
 297 [2007] predicts an occurrence frequency of a March 1989 storm intensity ($D_{ST} = -589nT$)
 298 or greater as once in 60 years. In Figure 4, 1989 is ranked the 5th most active year in 150
 299 years of *aa* observations, giving a return period of 30 years.

5 Conclusions

The *aa* index extends over the last 14 solar cycles, it is the longest almost continuous record of geomagnetic activity at the earth's surface. However the *aa* index is constructed from observations that are logarithmically discretized in amplitude and thus individual records of the 3 hour *aa* index will have uncertainties that are both significant and non-trivial to estimate [Bubenik & Fraser-Smith, 1977]; in particular its extreme excursions are not well resolved in amplitude. We parameterized extreme *aa* activity using averages of the annual top few % of observed records. Our analysis based on rank order plots [Sornette, 2003] shows that the distribution tail (of the top 100 annual estimates of extreme *aa* activity) is well described by an exponential distribution ($r > 0.99$). The D_{ST} index is available for the last five solar cycles and as its amplitude is well resolved it is commonly used to characterise the intensity of space weather events. We found a good correspondence ($r \sim 0.8$) between the annual minimum D_{ST} value and the annual averaged top few (0.5 %, 5%) values of *aa* over the last five solar cycles. This can be used to 'read across' between annual minimum D_{ST} values and extreme activity in *aa*.

We then find that least one 'severe' storm of $D_{ST} < -250nT$ occurred in each of 42 (~28% [20,35]) of those years and at least one 'great' storm $D_{ST} < -500nT$ occurred in each of 6 (~4% [0.9,7]) of those years. These estimates are an overall average and do not take into account any solar cycle phase variation. By sampling over 14 solar cycles, they do include a greater variety of solar cycle intensities than estimates that rely upon data from the last five cycles.

We extended this analysis to D_{ST} estimates for the Carrington event, to compare them with the annual level of extreme activity seen in *aa*. Extrapolating our exponential distribution gives an estimate $D_{ST} = -809$ [-663, -955] for a 1 in 151 year event that follows the same distribution as other extreme activity seen in *aa* over the last 14 solar cycles. The occurrence of a $D_{ST} \sim -850nT$ [Siscoe et al., 2006] event in a single year is consistent with this distribution tail. A Carrington event on this scale is a more intense version of the other super-storms that have occurred since 1868, so that in this case the set of observed super-storms can be used to predict how likely such an event is in the future. A $D_{ST} \sim -1760nT$ Carrington event on the other hand is far from the distribution tail and is in a class of its own, it is a 'Dragon King' [Sornette & Ouillon, 2012] requiring the concurrence of special conditions in the corona and solar wind and at the earth. The 2012 "solar storm" [Liu et al., 2012] is an event in this class, where the correlated dynamics of several CMEs created the conditions for an unusually intense event.

Acknowledgments

The results presented in this paper rely in part on geomagnetic indices calculated and made available by ISGI Collaborating Institutes from data collected at magnetic observatories. We acknowledge the involved national institutes, the INTERMAGNET network and ISGI (isgi.unistra.fr). We also acknowledge Lockwood et al. [2018b,c] for the provision of the homogenous *aa* index used here. We thank the World Data Center for Geomagnetism, Kyoto. We thank the World Data Center SILSO, Royal Observatory of Belgium, Brussels for provision of sunspot data.

SCC acknowledges a Fulbright-Lloyd's of London Scholarship and AFOSR grant FA9550-17-1-0054 and ST/P000320/1. RBH acknowledges the NERC Highlight topic grant NE/P01738X/1 (Rad-Sat) and NE/R016038/1.

Data availability: The ISGI *aa* index dataset analysed here was downloaded from the International Service of Geomagnetic Indices at <http://isgi.unistra.fr/>. The homogenized *aa* index analysed here was downloaded from the SI of Lockwood et al. [2018c] at <https://www.swsc-journal.org/articles/swsc/olm/2018/01/swsc180022/swsc180022.html>. The daily sunspot number dataset was downloaded from the SILSO, World Data Center -

350 Sunspot Number and Long-term Solar Observations, Royal Observatory of Belgium, on-
351 line Sunspot Number catalogue: <http://www.sidc.be/SILSO/>, '1868-2017' The D_{ST} index
352 analysed here was downloaded from NASA/GSFC's Space Physics Data Facility's OMNI-
353 Web service, the OMNI data were obtained from the GSFC/SPDF OMNIWeb interface at
354 <https://omniweb.gsfc.nasa.gov>.

References

- Baker, D. N., & Lanzerotti, L. J. (2016). Resource Letter SW1: Space weather, *Am. J. Phys.* 84, 166. <https://doi.org/10.1119/1.4938403>
- Bartels, J., Heck, N. H., Johnston, H. F. (1939) The three-hour-range index measuring geomagnetic activity, *J. Geophys. Res.*, doi:10.1029/TE044i004p00411
- Bubenik, D. M., Fraser-Smith, A. C., (1977) Evidence for strong artificial components in the equivalent linear amplitude geomagnetic indices, *J. Geophys. Res.*, 82, 2875
- Cannon, P., Angling M., Barclay, L., Curry, C., Dyer, C., Edwards, R., Greene, G., Hapgood, M., Horne, R. B., Jackson, D., Mitchell, C. N., Owen, J., Richards, A., Rodgers, C., Ryden, K., Saunders, S., Sweeting, M., Tanner, R., Thomson, A. and Underwood, C., (2013) *Extreme Space Weather: Impacts on Engineered Systems and Infrastructure*, pp. 1-68, Royal Academy of Engineering, London, United Kingdom.
- Chapman, S. C., Watkins, N. W., Tindale, E., (2018) Reproducible aspects of the climate of space weather over the last five solar cycles, *Space Weather*, doi:10.1029/2018SW001884
- Clicher, E. W., Svalgaard, L., (2004) The 1859 solar-terrestrial disturbance and the current limits of extreme space weather activity, *Solar Physics*, 224: 407-422
- Daglis, I. A. (ed.) (2004) *Effects of space weather on technology infrastructure*, pp. 1-334, Kluwer Academic Publishers, Dordrecht, The Netherlands.
- Elvidge, S., Angling, M. J. (2018). Using Extreme Value Theory for Determining the Probability of Carrington-Like Solar Flares. <https://doi.org/10.1002/2017SW001727>
- Feynman, J., (1982). Geomagnetic and solar wind cycles, 1900-1975, *J. Geophys. Res.*, 87(A8), 6153-6162. <https://doi.org/10.1029/JA087iA08p06153>
- Greenwood, M. (1926). *The Natural Duration of Cancer*, in *Reports of Public Health and Related Subjects*, Vol. 33, HMSO, London.
- Hathaway, D. H. (2015) The solar cycle, *Living Rev. Solar Phys.*, 12, 4. <https://doi.org/10.1007/lrsp-2015-4>
- Hayakawa H., et al. (2019) Temporal and Spatial Evolutions of a Large Sunspot Group and Great Auroral Storms around the Carrington Event in 1859, *Space Weather* <https://doi.org/10.1029/2019SW002269>
- Hush, P., S. C. Chapman, M. W. Dunlop, N. W. Watkins (2015), Robust statistical properties of the size of large burst events in AE, *Geophys. Res. Lett.*, 42, doi:10.1002/2015GL066277.
- Kelly, G. S., Viljanen, A., Beggan, C. D., Thomson, A. W. P., (2016) Understanding GIC in the UK and French high-voltage transmission systems during severe magnetic storms, *Space Weather*, 15, 99-114, doi: 10.1002/2016SW001469
- Lakhina G. S., Tsurutani B. T. (2016). Geomagnetic storms: historical perspective to modern view. *Geosci. Lett.* 3:5 DOI 10.1186/s40562-016-0037-4
- Liu, Y. D., Luhmann, J. G., Kajdic, P., E.Kilpua, K. J., Lugaz, N., Nitta, N. V.,östl, C. M., Lavraud, B., Bale, S. D., Farrugia, C. J., Galvin, A. B., (2014) Observations of an extreme storm in interplanetary space caused by successive coronal mass ejections, *Nat. Com.* 5, 3481 doi:10.1038/ncomms4481
- Lockwood, M., Owens, M. J., Barnard, L. A., Scott, C. J., Watt, C. E., Bentley, S., (2018a). Space climate and space weather over the past 400 years: 2. Proxy indicators of geomagnetic storm and substorm occurrence, *J. Space Weather Space Climate*, 8, A12. <https://doi.org/10.1051/swsc/>
- Lockwood, M., A. Chambodut, L.A. Barnard, M.J. Owens, and E. Clarke (2018b) A homogeneous aa index: 1. Secular variation, *J. Space Weather Space Climate*, doi: 10.1051/swsc/2018038
- Lockwood, M., I.D. Finch, A. Chambodut, L.A. Barnard, M.J. Owens, and E. Clarke (2018c) A homogeneous aa index: 2. hemispheric asymmetries and the equinoctial variation, *J. Space Weather Space Climate*

- 407 Love, J. J., Rigler, E. J., Pulkkinen, A. and Riley, P., (2015). On the lognormality of his-
 408 torical magnetic storm intensity statistics: Implications for extreme-event probabilities,
 409 *Geophys. Res. Lett.*, 42(16), 6544-6553, doi:10.1002/2015GL064842
- 410 Love, J. J., (2018) The Electric Storm of November 1882. *Space Weather*, 16,
 411 doi:10.1002/2017SW001795.
- 412 Love, J. J., Coïsson, P., (2016) The Geomagnetic Blitz of September 1941, *Eos*. 97.
 413 doi:10.1029/2016EO059319.
- 414 Love, J. J., Hayakawa, H., & Cliver, E. W. (2019). On the intensity of the magnetic super-
 415 storm of September 1909. *Space Weather*, 17, 37-45. doi:10.1029/2018SW002079
- 416 Love, J. J., Hayakawa, H., Cliver, E. W. (2019). Intensity and impact of the
 417 New York Railroad superstorm of May 1921. *Space Weather*, 17, 1281–1292.
 418 <https://doi.org/10.1029/2019SW002250>
- 419 MacNeil, J. (2018) Solar explosion leads to blackout, March 10, 1989. EDN Network,
 420 March 10
- 421 Mayaud, P-N. (1972) The aa indices: A 100 year series characterizing the magnetic activ-
 422 ity, *J. Geophys. Res.*, 77, 6870
- 423 Mayaud, P. N. (1980). Derivation, Meaning, and Use of Geomagnetic Indices, *Geophys.*
 424 *Monogr. Ser.*, vol. 22, AGU, Washington, D.C. <https://doi.org/10.1029/GM022>
- 425 Oughton, E. J., A. Skelton, R. B. Horne, A. W. P. Thomson, and C. T. Gaunt (2017),
 426 Quantifying the daily economic impact of extreme space weather due to failure in elec-
 427 tricity transmission infrastructure, *Space Weather*, 15, doi:10.1002/2016SW001491.
 428 <https://doi.org/10.1007/s11207-018-1330-5>
- 429 Riley, P. (2012). On the probability of occurrence of extreme space weather events, *Space*
 430 *Weather* 10, S02012.
- 431 Riley, P., Love, J. J., (2016) Extreme geomagnetic storms: Probabilistic forecasts and their
 432 uncertainties, *Space Weather*, 15, 53-64, doi:10.1002/2016SW001470.
- 433 Silverman S. M. and Cliver E. W., (2001) Low-latitude auroras: the magnetic storm of
 434 14-15 May 1921. *Journal of Atmospheric and Solar Terrestrial Physics*, 63(5):523-535.
- 435 Silbergleit, V. M. (1996). On the occurrence of geomagnetic storms with sudden com-
 436 mencements, *J. Geomagn. Geoelectr.*, 48, 1011.
- 437 Silbergleit, V. M. (1999). Forecast of the most geomagnetically disturbed days, *Earth Plan-*
 438 *ets Space*, 51, 19. <https://doi.org/10.1186/BF03352205>
- 439 Siscoe, G. L. (1976). On the statistics of the largest geomagnetic storms per solar cycle, *J.*
 440 *Geophys. Res.*, 81, 4782. <https://doi.org/10.1029/JA081i025p04782>
- 441 G. Siscoe, N. U. Crooker, C. R. Clauer, (2006) D_{st} of the Carrington storm of 1859, *Adv.*
 442 *Space. Res.* 38, 173-179
- 443 Sornette, D. (2003) *Critical phenomena in natural sciences*, 2nd Ed. Springer
- 444 Sornette, D., Ouillon, G., (2012) Dragon-kings: mechanisms, statistical methods and em-
 445 pirical evidence. *The European Physical Journal Special Topics* 205.1 1-26
- 446 Sugiura, M., (1964) Hourly value of equatorial Dst for the IGY, *Ann. Int. Geophys. Year*,
 447 35, 9-45.
- 448 Sugiura, M. & Kamei, T., (1991) Equatorial Dst index 1957-1986, *IAGA Bull.*, 40, ISGI
 449 Publication Office, Saint-Maur-des-Fosses, France.
- 450 Thomson, A. W. P., Gaunt, C. T., Cilliers, P., Wild, J. A., Opperman, B., McKinnell, L.-
 451 A., Kotze, P., Ngwira, C.M., Lotz, S.I., Present day challenges in understanding the
 452 geomagnetic hazard to national power grids (2010) *Adv. Space Res.* 45 1182-1190
 453 doi:10.1016/j.asr.2009.11.023
- 454 Thomson, A. W. P., Dawson, E. B., Reay, S. J. (2011). Quantifying extreme behaviour in
 455 geomagnetic activity, *Space Weather*, 9, S10001. <https://doi.org/10.1029/2011SW000696>
- 456 Tindale, E., S. C. Chapman (2016), Solar cycle variation of the statistical distribution
 457 of the solar wind ϵ parameter and its constituent variables, *Geophys. Res. Lett.*, 43,
 458 doi:10.1002/2016GL068920.

- 459 Tindale, E., Chapman, S. C. (2017). Solar wind plasma parameter variability across so-
460 lar cycles 23 and 24: From turbulence to extremes. *Journal of Geophysical Research:*
461 *Space Physics*, 122. <https://doi.org/10.1002/2017JA024412>
- 462 Tsubouchi, K., Omura, Y. (2007). Long-term occurrence probabilities of intense geomag-
463 netic storm events, *Space Weather*, 5, S12003. doi: 10.1029/2007SW000329
- 464 Tsurutani, B. T., Gonzalez, W. D., Lakhina, G. S., Alex, S., (2003) The extreme
465 magnetic storm of 1-2 September 1859, *J. Geophys. Res.*, 108(A7), 1268,
466 doi:10.1029/2002JA009504
- 467 Tsurutani, B. T., et al. (2006) Corotating solar wind streams and recurrent geomagnetic
468 activity: A review, *J. Geophys. Res.*, 111, A07S01, doi:10.1029/2005JA011273.
- 469 Weaver, M., Murtagh, W., et al. (2004) Halloween Space Weather Storms of 2003, NOAA
470 Technical Memorandum. OAR SEC-88. Boulder, CO: Space Environment Center.
471 OCLC 68692085
- 472 World Data Center for Geomagnetism, Kyoto, M. Nose, T. Iyemori, M. Sugiura, T. Kamei
473 (2015), Geomagnetic Dst index, doi:10.17593/14515-74000.